CALIFORNIA STATE UNIVERSITY, NORTHRIDGE

PROTEIN FOLDING: PLANAR CONFIGURATION SPACES OF DISC ARRANGEMENTS AND HINGED POLYGONS

A thesis submitted in partial fulfillment of the requirements for the degree of
Master of Science in Applied Mathematics

by

Clinton Bowen

August 2014

The thesis of Clinton Bowen is approved:

Dr. Silvia Fernandez	Date
Dr. John Dye	Date
Dr. Csaba Tóth, Chair	Date

California State University, Northridge

Table of Contents

ABSTRACT

PROTEIN FOLDING: PLANAR CONFIGURATION SPACES OF DISC ARRANGEMENTS AND HINGED POLYGONS

By

Clinton Bowen

Master of Science in Applied Mathematics

Chapter 1

Realizability of Polygonal Linkages with Fixed Orientation

We begin the chapter with describing several gadgets that translates the associated graph $A(\Phi)$ of a P3SAT boolean formula. These gadgets will be used together to form a special hexagonal tiling that behaves in a similar nature to the logic engine that encoded a NAE3SAT instance of Chapter **??** but instead encodes a Planar 3-SAT and its associated graph. Together the gadgets will form what is called the auxilary construction. A hexagonal tiling and several gadgets enclosed in a frame (a frame that is conceptually similar to the frame found in a logic engine) would then be used to prove the following theorem:

Theorem 1. *It is strongly NP-hard to decide whether a polygonal linkage whose hinge graph is a **tree** can be realized with counter-clockwise orientation.*

Our proof is a reduction from P3SAT. Given an instance Φ of P3SAT with n variables and m clauses and its associated graph $A(\Phi)$, we construct a simply connected polygonal linkage $(\mathscr{P},H)$, of polynomial size in n and m, such that Φ is satisfiable if and only if $(\mathscr{P},H)$ admits a realization with fixed orientation.

We construct a polygonal linkage in two main steps: first, we construct an auxiliary structure where some of the polygons have fixed position in the plane (called *obstacles*), while other polygons are flexible, and each flexible polygon is hinged to an obstacle. Second, we modify the auxiliary construction into a polygonal linkage by allowing the obstacles to move freely, and by adding new polygons and hinges as well as an exterior *frame* that holds the obstacle polygons in place. All polygons in our constructions are regular hexagons or long, skinny rhombi. In Chapter **??** we can "simulate" these shapes with disk arrangements to show related results.

Storer, Tamassia, and Tollis showed that if $G=(V,E)$ is planar, it can be embedded in an $|V|\times|V|$ grid with $S(G)=2.4|V|+4$ bends [1, 2]. Note that this result implies that a planar graph can be embedded in a grid of size $S(G)\times S(G)$; and this allows $S(G)$ to act as a fundamental polynomial problems with planar graphs defined in a embedding in a grid. We can define a *bend polynomial*, $s(n,m)$ that will be used to construct our gadgets which will be used to prove Theorem 1. For our constructions, our bend polynomial can be any polynomial strictly greater than $S(G)$, e.g.:

$$6(n+m)+4.$$

The table below is a glossary of formulas that are used to throughout this chapter. It will serve as a useful reference for the reader.

$z(n,m)$	$=$	$4s(n,m)$
$J_h(z)$	$=$	$6z(n,m)+1=24s(n,m)+1$
$J_d(z)$	$=$	$4z(n,m)+1=16s(n,m)+1$
$N(n,m)$	$=$	$\frac{5t-1}{2}=\frac{5s^{\kappa}-1}{2}$
$t(n,m)$	$=$	s^{κ}
$H(n,m)$	$=$	$(12s+1)(5t-1)\sqrt{3}+12s\left(\sqrt{3}+\frac{1}{250t-50}\right)$
$\tan^{-1}x$	$\approx$	x
$\sin x$	$\approx$	x
$\cos x$	$\approx$	$1-\frac{x^2}{2}$
$\sec x$	$\approx$	$1-\frac{x^2}{2}$

The formula $t(n,m) = s^{\kappa}$ has an exponent κ which is a sufficiently large integer that is chosen later on so that all arguments in this chapter are satisfied. The trigonmetric functions in the table above each are expressed as either the first term or the first and second term of their Maclaurin Series expansion.

Modifying the Associated Graph of a P3SAT. Given an instance of P3SAT boolean formula Φ of n variables and m clauses with associated graph $A(\Phi)$, we construct a finite *honeycomb* grid $H_{A(\Phi)}$ of regular hexagons over the plane centered at origin. We modify the associated graph drawing $A(\Phi)$ by overlaying it onto a honeycomb in the following way:

1. **Variable:** A vertex representing a variable shall encompass a consecutive set of hexagons along a horizontal line in the honeycomb (see Figure 1.1).

   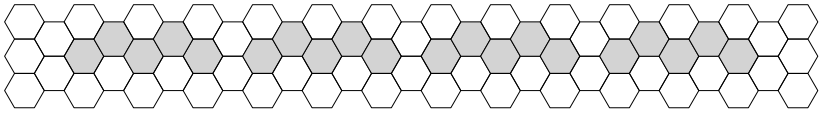

   Figure 1.1: The four shaded groups of horizontally adjacent hexagons represent four distinct variables from a boolean formula in the honeycomb.

   Let $D = \max_{v \in V} \deg(v)$ where V is the set of vertices of $A(\Phi)$. Every variable vertex v must encompass at least $2 \cdot \deg(v)$ consecutive hexagons but can encompass up to $2 \cdot D$ consecutive hexagons.

2. **Clause:** A vertex representing a clause shall be a vertex of a hexagon in the honeycomb.

3. **Edge:** Edges of the associated graph $A(\Phi)$ are paths between the variable x_i and clause C_j. An edge $\{x_i, C_j\}$ of the associated graph is pariwise edge disjoint. The edges of the drawing shall traverse the edges of hexagons in a vertically or horizontally zigzagging manner (see Figure 1.2) in the honeycomb from the literal to the corresponding clause. Edges traverse a hexagon in two edges vertically, three edges horizontally. The vertical zigzagging edge segments traverse the left or right sides of a hexagon(s). The horizontal zigzagging edge segments traverse the top or bottom halves of a hexagon(s). When the edge transisitions from a vertical to horizontal traversal, the edge traverses in over 4 edges about the hexagon. The length of the edges are bounded above by $6 \cdot (\ell_1(x_i, C_j) + D)$ where ℓ_1 is the L_1 norm.

Figure 1.2 illustrates an associated graph of a P3SAT overlayed on a honeycomb. This type of construction emulates an *orthoganal drawing* over a hexagonal grid; an orthoganal drawing where edges are drawn with alternating vertical and horizontal line segments. Let the region in which the construction lies in be a regular hexagon region with polynomial side length $s(n,m)$.

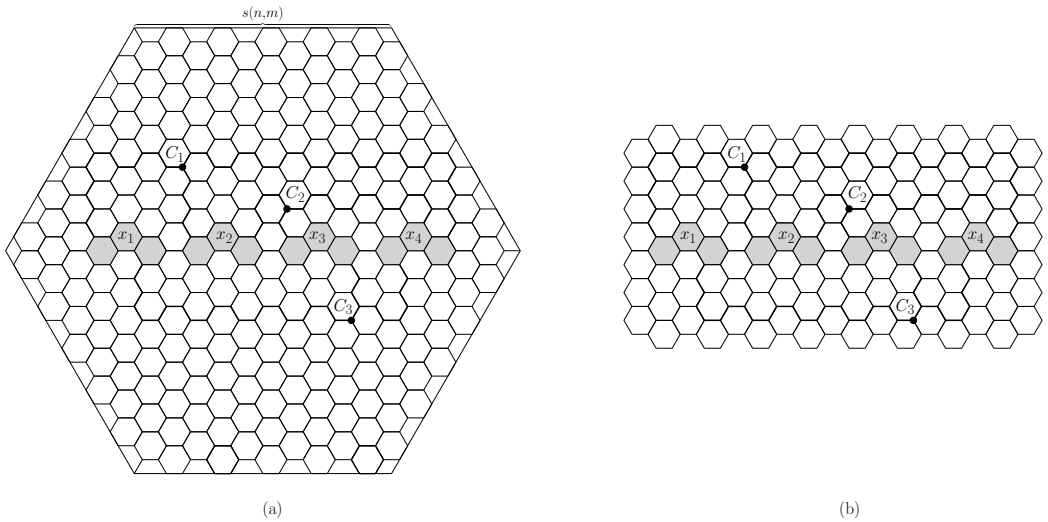

Figure 1.2: (a) This is an instance of an associated graph for a P3SAT overlayed onto a honeycomb grid and placed into a regular hexagonal region. This honeycomb graph could correspond to Boolean formula $(\neg x_1 \vee \neg x_2 \vee x_4) \wedge (x_2 \vee \neg x_3 \vee x_4) \wedge (x_1 \vee \neg x_3 \vee \neg x_4)$. (b) This is the same instance as (a) shown without the hexagonal region.

The honeycomb construction will act as preliminary concept that will be refined further in the Auxilary Contruction.

1.1 Auxilary Construction

Let Φ be a Boolean formula of P3SAT with variables $x_1, \ldots, x_n$ and clauses $C_1, \ldots, C_m$, where $A(\Phi)$ is the associated planar graph and $\tilde{A}(\Phi)$ be corresponding honeycomb graph. We continue to modify $\tilde{A}(\Phi)$ to form the auxilary construction. Consider a large (polynomial-size) regular hexagon J with side length $s(n,m)$ that contains all gadgets in our construction and hexagonal grid. For each hexagon of the hexagonal grid contained in J, scale the hexagon in the following way: first we fix the center of the hexagon and then scale (shrink) the hexagon; adjacent hexagons in the honeycomb no longer touch each other and form corridors and junctions between the hexagons (See Figure 1.3).

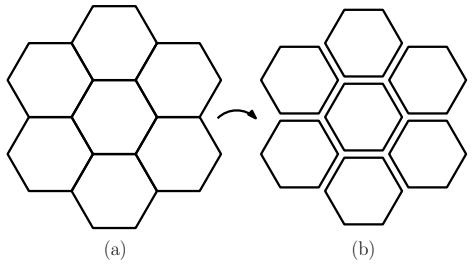

Figure 1.3: (a) This figure shows a region of a hexagonal grid scaled in place to form corridors between adjacent hexagons(shown in (b)).

Formally, let a *corridor* be a channel between two adjacent hexagons and a *junction* be a region where three corridors meet.

Formal Decscription of the Auxilary Construction. Given the side length of J, $s(n,m)$, we need to scale the grid of hexagons of the hexagonal grid in the interior of J accordingly.

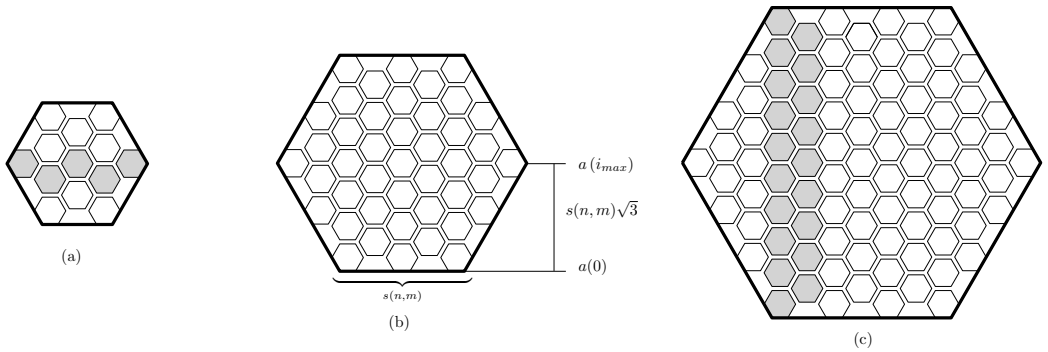

Figure 1.4: (a) shows a *formal auxilary construction* with $k = 2$. k is the number of hexagons of the hexagonal grid in the interior of J that is on the bottom most row. (b) shows a formal auxilary construction with $k = 3$. (c) shows a formal auxilary construction with $k = 4$. Note that in each figure

In Figure 1.4, we show the three smallest possible formal constructions of J, J_1, J_2, J_3. A *formal construction* of J is when six hexagons of the hexagonal grid each have two adjacent lie on the perimeter of J. We have shown informal construction earlier where this does not occur. Unless otherwise specified, we will assume the use formal constructions. Each of the figures in Figure 1.4 shows J in bold and the hexagonal grid in its interior. Notice that in each case we have six hexagons of the hexagonal grid with each of the six hexgaons having two adjacent sides that lie on the perimeter of J.

The height and diamater of J can be described by the number of hexagons in the grid a vertical or horizontal line may cross. We'll denote these qualities as the hexagonal height and hexagonal diameter of J. Figure Figure 1.4(c) and Figure 1.4(a) show the hexagons of the hexagonal height and hexagonal diamters of J_1 and J_3 respectively. The formula for calculating hexagonal height of J_z is

$$J_h(z) = 6z + 1 \tag{1.1}$$

The formula for calcuating the hexagonal diameter of J_z is

$$J_d(z) = 4z + 1 \tag{1.2}$$

If an associated graph of a P3SAT instance can be encoded into a honeycomb grid of size $s(n,m) \times s(n,m)$, then let $z(n,m) = 4 \cdot s(n,m)$ to enclose the same honeycomb to be enclosed into the interior of J_z.

Figure 1.4(b) illustrates the side length of J as $s(n,m)$ and half the height of J as $s(n,m)\sqrt{3}$. For any J, there is a fixed number of hexagons in the hexagonal grid that lie on one side of the perimeter of J; denote this number as k. We can denote the number of hexagons in a row of the hexagonal grid in J_z with the following sequence as follows:

$$\begin{aligned} a(0) &= k \\ a(1) &= k-1 \\ a(2) &= k \\ a(i) &= a(i-3)+1 \\ 0 \leq\ & i \leq \left\lceil \tfrac{J_h(z)}{2} \right\rceil \end{aligned} \tag{1.3}$$

The i^{th} number of Sequence 1.3 indicates the number of hexagons on the i^{th} row of the hexagonal grid in the interior of J from the perimeter of J up to the half height of J. In Figure 1.4(c) from the bottom to the mid-height of J, the sequence $a(i)$ (i.e. the number of hexagons in each subsequent row) is 4, 3, 4, 5, 4, 5, 6, 5, 6, 7. Denote the hexagons of the hexagonal grid in J as *obstacle hexagons*.

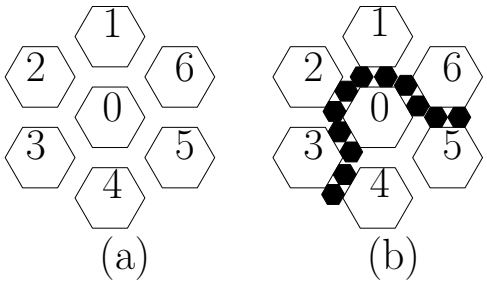

Figure 1.5: (a) A region of the honeycomb shown with scaling. The corridors and junctions formed from the first scaling is preserved after scaling the honeycomb grid to where the side lengths of the hexagon are $N(n,m)$. (b) The same region in (a) containing flags.

Let the numbered hexagons of Figure 1.5(a) be obstacle hexagons that are fixed. In Figure 1.5(b), we have smaller hexagons within some corridors and junctions. These hexagons are flags. For each edge in $\tilde{A}(\Phi)$, we insert flags into the corridor corresponding to that edge. Flexible hexagons are hinged at the vertex closest to origin and the side of the corridor (See Figure 1.6). Let $t(n,m) = s^{\kappa}$ be the number of flags in a corridor (see Figure 1.6). Scale J and the obstacle hexagons in the interior of J independently from their centers (see Figure 1.3) such that each obstacle hexagon has side length:

$$N(n,m) = \frac{5t(n,m)-1}{2}.$$

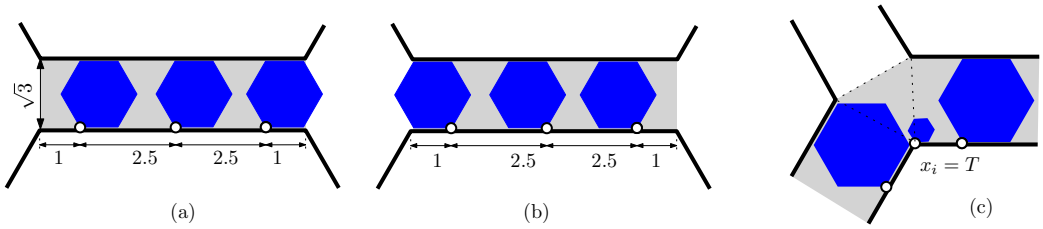

Figure 1.6: (a) A corridor when all unit hexagons are in state R. (b) A corridor where all unit hexagons are in state L. (c) A junction where a small hexagon between two corridors ensures that at most one unit hexagon enters the junction from those corridors.

Between two adjacent obstacle hexagons, there is a $\frac{5t-1}{2} \times \sqrt{3}$ rectanglar corridor. Three adjacent corridors meet at a regular triangle, which we call a junction. For each corridor, there are two junctions adjacent to it; of these two junctions, we denote the junction from which a flag in the corridor enters into as the *active junction* (see Figure 1.7).

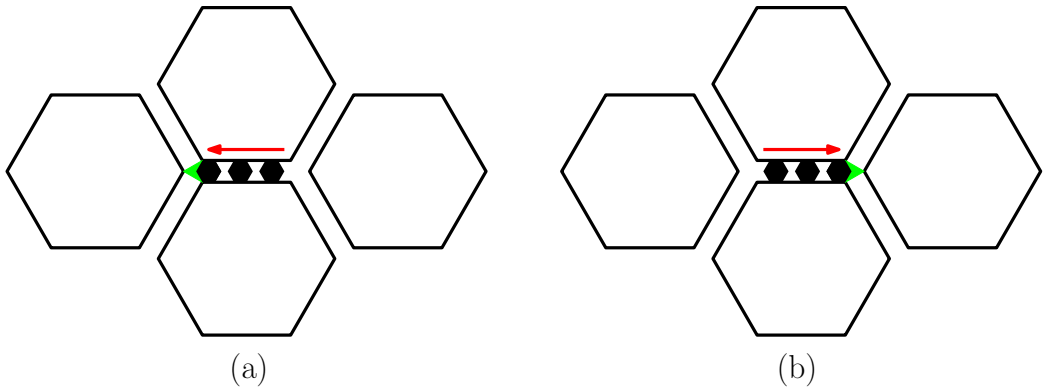

Figure 1.7: The active junction in (a) is the junction on the left and in (b) the active junction is on the right. The active junction is the junction in which a flag enters from a corridor.

We next describe variable, clause, and transmitter gadgets. The basic building block of both variable and transmitter gadgets consists of t regular hexagons of side length 1 (*unit hexagons*, for short) attached to a wall of a corridor such that the hinges divide the wall into $t+1$ intervals of length $(1, 2.5, \ldots, 2.5, 1)$ as shown in Fig. 1.6(a-b).

In some of the junctions, we attach a small hexagon of side length $\frac{1}{3}$ to one or two corners of the junction (see Fig. 1.6(c) and Fig. 1.11).

Variable Gadget. The **variable gadget** for variable x_i is constructed as follows. Recall that variable x_i corresponds to a cycle in the associated graph $\tilde{A}(\Phi)$, which has been embedded as a cycle in the hexagonal tiling, with corridors and junctions. In each junction along this cycle, attach a small hexagon in the common boundary of the two corridors in the cycle. Figure 1.8 depicts a *variable gadget* in the hexagonal grid.

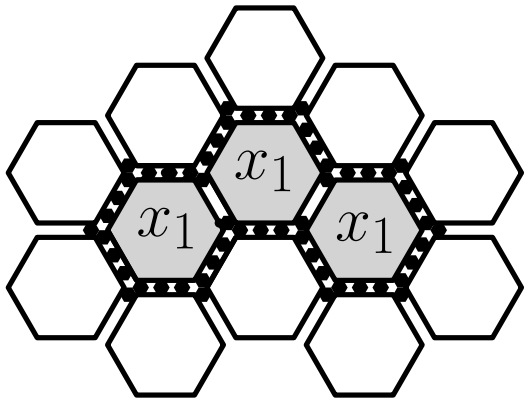

Figure 1.8: This depicts a variable gadget with $x_1 = T$. Carefully note that the flags around x_1 are in the state R. Corridors adjacent to two obstacles of a variable in the honeycomb do not have t flags; these corridors simply have the flexible hexagons at the junctions.

Clause Gadget. Recall that a clause from a Boolean formula Φ in 3-CNF has three literals. If Φ is a 'yes' instance, then at least one literal in every clause of Φ is true. We construct the clause gadget to model this fact about Boolean formulas in 3-CNF.

The **clause gadget** lies at a junction adjacent to three transmitter gadgets (see Fig. 1.9 and Section 1.1). At such a junction, we attach a unit line segment to an arbitrary vertex of the junction, and a small hexagon of side length $\frac{1}{3}$ to the other end of the segment. If unit hexagons enter the junction from all three corridors

(i.e., all three literals are false), then there is no space left for the small hexagon.

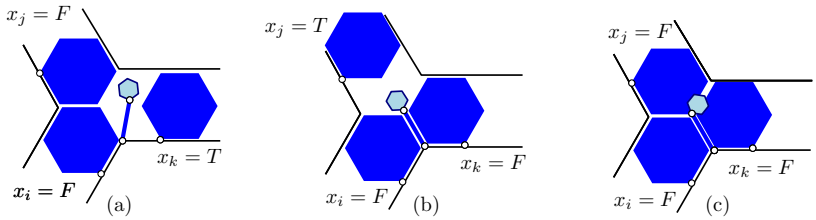

Figure 1.9: (a-b) A clause gadget $(x_i \vee x_j \vee x_k)$ is realizable when at least one of the literals is TRUE. (c) The clause gadget cannot be realized when all three literals are FALSE.

But if at most two unit hexagons enter the junction (i.e., one of the literals is true), then the unit segment and the small hexagon are realizable.

Transmitter Gadget. In the planar 3-SAT graph $A(\Phi)$, every variable vertex has an associated cyclic order of edges. Suppose we have a variable vertex x_i with counter-clockwise cyclic order of edges $(\{x_i, C_1\}, \{x_i, C_2\}, \ldots, \{x_i, C_k\})$. Assign distinct junctions of the variable cycle of x_i to the edges $\{x_i, C_j\}$ in the same cyclic order (refer to Figure 1.10 for an example).

A **transmitter gadget** is constructed for each edge $\{x_i, C_j\}$ of the graph $A(\Phi)$; it consists of a sequence of junctions and corridors from a variable gadget's junction to a clause junction.

For each junction in the transmitter gadget, we attach a small hexagon in the junction as shown in Figure 1.11 except at the clause junction. Choosing the location of the small hexagon depends on whether the non-negated or negated literal is found in the clause.

(a) For an edge (x_i, C_j) of the graph $A(\Phi)$, if the non-negated literal of x_i exists in C_j, attach the small hexagon to the left side of the junction (see Figure 1.10(a)).

(b) For an edge (x_i, C_j) of the graph $A(\Phi)$, if the negated literal of x_i exists in C_j, attach thhe small hexagon to the right side of the junction (see Figure 1.10(b)).

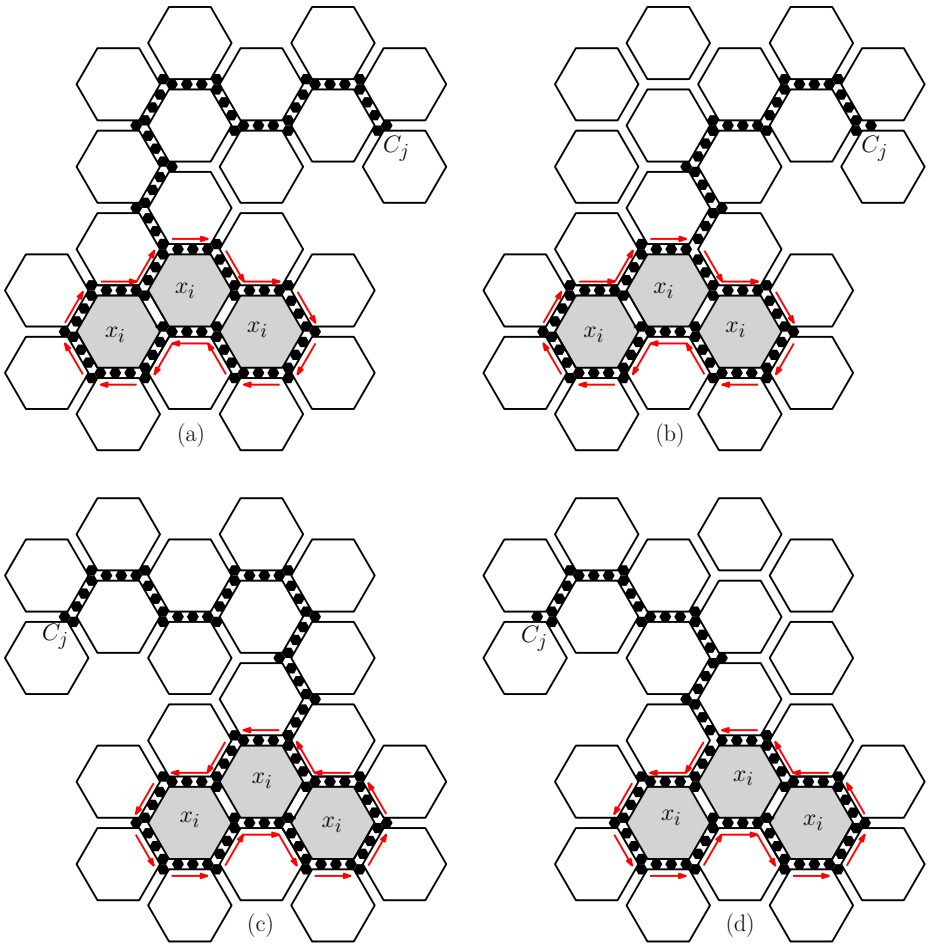

Figure 1.10: These four figures depict an example of placing a transmitter gadget corresponding to edge $\{x_i, C_j\}$.

Figure 1.10 shows an example of each rule on choosing a junction to attach a transmitter gadget. The first column transmits a "true" value between the variable gadget and clause junction. The second column transmits a "false" value between the variable gadget and clause junction. The variable gadgets in the first row are are in state R, i.e. variable $x_i = T$. The variable gadgets in the second row are are in state L, i.e. variable $x_i = F$.

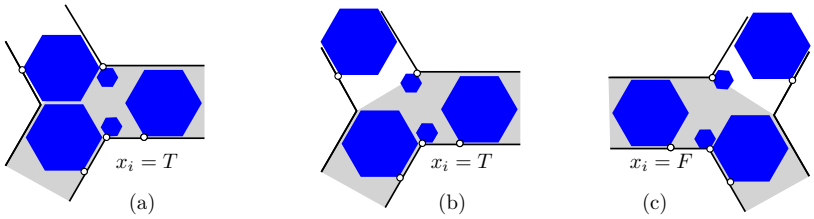

Figure 1.11: The common junction of a variable gadget and a transmitter gadget. (a) When $x_i = T$, a hexagon of the transmitter may enter the junction of the variable gadget. (b) When $x_i = T$, the transmitter gadget has several possible realizations. (c) When $x_i = F$, no hexagon from the transmitter enters a junction of the variable gadget.

1.1.1 Functionality of the Auxilary Construction and Gadgets

If the literal x_i (resp., $\bar{x}_i$) appears in C_j, then we attach a small hexagon to the corner of this junction such that if $x_i = F$ (resp., $\bar{x}_i = F$), then the unit hexagon of the transmitter gadget cannot enter this junction.

A variable gadget for vertex v in the associated graph of a P3SAT Boolean formula encompasses at least $2 \cdot \deg(v)$ consecutive obstacle hexagons. The arrangement of the consecutive obstacle hexagons are in staggered fashion about a horizontal line where there are at least $\deg(v)$ obstacle hexagons in the upper portion of the staggering arrangement and at least $\deg(v)$ obstacle hexagons in the lower portion of the staggering arrangement.

Section 1.1 is a formal description of the auxilary construction and its gadgets. This subsection covers the underlying assumptions and proofs about the functionality of the auxilary construction. The first observations about the functionality of the auxilary construction are about the flags.

Observation 1. (1) If the leftmost hexagon is in state R, then all t hexagons are in state R, and the rightmost hexagon enters the junction on the right of the corridor.

(2) Similarly, if the rightmost hexagon is in state L, then all t hexagons are in state L, and the leftmost hexagon enters the junction on the left of the corridor.

Observation 1 and the small hexagons ensure that the state of any unit hexagon along the cycle determines the state of all other unit hexagons in the cycle. This property defines the binary variable x_i: If $x_i = T$, then all unit hexagons in the top horizontal corridors are in state R; and if $x_i = F$, they are all in state L.

When a binary variable $x_i = T$, we will say that the variable in state R and that the cycle of small hexagons around the variable gadget are in a "clockwise direction". When a binary variable $x_i = F$, we will say that the variable is in state L and that the cycle of small hexagons around the variable gadget are in a "counter-clockwise direction".

The proof of the Observation 1 is similar to the proof of Lemma **??** regarding a row in a logic engine having a collision-free configuration.

Proof. Suppose the leftmost hexagon, h_1, is in state R in a corridor. Denote the t flags in a corridor as h_1, h_2, …, h_t from leftmost to rightmost respectively. h_2 must be in state R otherwise we result in a collision between h_1 and h_2. Without losss of generality, h_i and h_{i+1} must be in a state R in order to prevent an adjacent flag collision. This implies that rightmost flag h_t must also be in state R; this implies that h_t enters the junction that is on the right of the corridor.

Similarly, suppose the rightmost hexagon, h_t, is in state L in a corridor. Denote the t flags in a corridor as h_1, h_2, …, h_t from leftmost to rightmost respectively. h_{t-1} must be in state L otherwise we result in a collision between h_t and h_{t-1}. Without losss of generality, h_i and h_{i+1} must be in a state L in order to prevent an adjacent flag collision. This implies that rightmost flag h_1 must also be in state L; this implies that h_1 enters the junction that is on the left of the corridor. □

The flags of the auxilary construction help communicate the boolean value of a variable gadget to the rest of the auxilary construction. This communication property of the flags in a corridor is analagous to the flags in a row of a logic engine.

Each junction is a regular triangle, adjacent to three corridors. In some of the junctions, we attach a small hexagon of side length $\frac{1}{3}$ to one or two corners of the junction (see Fig. 1.6(c) and Fig. 1.11). Importantly, we have the following observation:

Observation 2. If a small hexagon is attached to a vertex at a junction between two adjacent corridors, then a flag can enter the junction from at most one of those corridors.

Proof. Suppose there is a small hexagon attached to a vertex at a junction between two adjacent corridors. Suppose it is not that case that a flag can enter the junction from at most one of these adjacent corridors. Then there are two flags entering the junction, one from each adjacent corridor. The angular sum of the vertex about the adjacent corridors consists of the obstacle hexagon, both flags, and the small unit hexagon. Each angle of each hexagon is $\frac{2\pi}{3}$ radians, totalling to an angular sum of $\frac{8\pi}{3} > 2\pi$. This is a contradiction with the total angular sum of a vertex on the plane to be 2π. □

Observation 1 and the small hexagons ensure that the state of any unit hexagon along the cycle determines the state of all other unit hexagons in the cycle. This property defines the binary variable x_i: If $x_i = T$, then all unit hexagons in the top horizontal corridors are in state R; and if $x_i = F$, they are all in state L.

Suppose there is an edge $\{x_i, C_j\}$ in the graph $A(\Phi)$.

Lemma 1. *If $x_i = T$ and its negated literal is in C_j, then a flag enters into the clause gadget of C_j, otherwise it need not enter; if $x_i = F$ and its non-negated literal is in C_j, then a flexible hexagon enters into the clause gadget of C_j, otherwise it need not enter.*

Proof. The transmitter gadget for each literal is placed on an active junction of the variable gadget. This junction is "activated" by the variable gadget. By Observation 2, the flag nearest of the transmitter gadget to the variable gadget does not enter the transmitter-variable junction. By Observation 1 and the state of the flag nearest of the transmitter gadget to the variable gadget implies that the flags in that transmitter corridor activate the junction opposite the transmitter-variable junction. The subsequent flags in the transmitter gadget corridors have the same state of the flag in the transmitter gadget nearest of the transmitter-variable junction by Observations 1 and 2. This activation process continues up to the clause junction and the flag in the transmitter gadget nearest the clause junction enters the clause junction. □

Lemma 2. *Hexagons in a clause junction have a non-overlapping placement if and only if at least one of the three literals is true.*

Proof. Suppose we have a hexagons in a clause junction that have a non-overlapping placement. To show that there is at least one of the three literals is true, we do a proof by contradiction. Suppose all literals of the clause are false. If all literals of the clause are false, then all flags in each transmitter gadget nearest their clause junction enters the clause junction, as shown in Figure 1.9(c) which show the small hexagon overlapping flags in the clause junction, a contradiction with hexagons in the clause junction have a non-overlapping placement.

If at least one of the three literals is true, then by Lemma 1, this literal's flag need not enter the transmitter-variable junction. There allows for the small hexagon in the clause junction to move into the area where this literal's flag could enter the junction and thus allow non-overlapping placement of hexagons in the junction. □

For a variable gadget x_i, place horizontal axis h at mid-height of the gadget. Then we have the following lemma:

Lemma 3. *If variable $x_i = T$, then all flags above h are in state R and all flags below h are in state L; if variable $x_i = L$, then all flexible hexagons above h are in state L and all flexible hexagons below h are in state R.*

Proof. Suppose we have two adjacent corridors k_i and k_{i+1} sharing junction J_i and without loss of generality, k_i is the left most corridor. Observation 2 implies that there can only be one hexagon entering J_i from either k_i or k_{i+1}. If the hexagon that enters J_i is from corridor k_i, then this hexagon has state R and all flags in corridor k_i are in state R by Observation 1. Since the nearest flag of corridor k_{i+1} cannot enter the junction J_i, it must also have state R. All flags in corridor k_{i+1} are in state R by Observation 1.

The argument is similar if the hexagon entering J_i is from corridor k_{i+1} and all flags in both corridors k_i and k_{i+1} have state L.

Because variable gadgets form a simple cycle of corridors and junctions $(k_1, J_1, k_2, J_2, \ldots, k_n, J_n)$ and the argument above, all flags about a variable gadget have the same state. □

Lemma 4. *For every instance Φ of P3SAT, the above polygonal linkage with flexible and obstacle polygons has the following properties: (1) it has polynomial size; (2) its hinge graph is a forest; (3) it admits a realization such that the obstacle polygons remain fixed if and only if Φ is satisfiable.*

Proof. (1) We can bound the number of obstacle hexagons to represent a variable gadget by $2D$, where $D = (\max_{v \in V} \deg(v))$. The number of clause junctions is n. To give an upper bound on the number of flags in the auxiliary construction, we have to account for the flags in the transmitter gadgets, the extra hexagons found in junctions, and the flexible hexagons around the variable gadgets.

Recall that that the number of flags in a corridor are $t = 2N(m,n)^3 + 1$ where $N(m,n)$ is a polynomial. Recall that the drawing of $A(\Phi)$ have edges drawn in vertically and horizontally and can join at some "elbow". The distance can be measured in the ℓ_1 norm. Similarly in the honeycomb construction, the flexable hexagons zig-zig vertically and horizontally through out honeycomb. The number of corridors about an obstacle hexagon is 6. To give a generous upper bound on the number of flags in a transmitter gadget, is $6 \cdot t \cdot \ell_1(v_i, C_j)$, assuming each obstacle hexagon is of unit height.

The number of junctions in the auxiliary construction is the number of junctions to form all variable gadgets, transmitter gadgets, and clause gadgets. We know there are at most $2 \cdot D$ obstacle hexagons to form each variable gadget and 6 junctions for each obstacle hexagon. Therefore an upper bound for the number of flags around variable gadgets is $m \cdot 6 \cdot t \cdot 2 \cdot D$. The upper bound for the number of junctions in a transmitter gadget is $6\ell_1(v_i, C_j)$. Thus, the upper bound of all junctions in all transmitter gadgets is

$$6 \cdot \sum_{\{v_i, C_j\} \in E} \ell_1(v_i, C_j).$$

The upper bound on the total number of flags is

$$m \cdot 6 \cdot t \cdot 2 \cdot D + 6 \cdot \sum_{\{v_i, C_j\} \in E} \ell_1(v_i, C_j).$$

(2) Recall that a forest is a disjoint union of trees. By construction, each flag is hinged to exactly one obstacle hexagon. There are no hinges between obstacle hexagons. Consequently, each component of the hinge graph is a star, where the center corresponds to an obstacle hexagon and the leafs corresponds to the flexable hexagons attached to it.

(3) The final statement is to show an if and only if statement: it admits a realization such that the obstacle polygons remain fixed if and only if Φ is satisfiable.

Suppose Φ is satisfiable. Each variable has a boolean value and we can encode the corresponding auxilary construction accordingly. For each variable, we encode the boolean value by the state of the flags surrounding the variable gadget to R or L. Lemma 3 shows that the corridors and junctions around the variable gadget are realizable. Lemma 1 also show that for each transmitter gadget, every corridor and junction are also realizable. Lemma 2 shows that there is at least one hexagon in the clause junction and that the clause is realizable. Thus all parts of the auxilary construction realizable and thus we have a realization.

Suppose the construction admits a realization such that the obstacle polygons remain fixed. Each variable gadget's flags are configured to state L or R. The variable's corresponding state correspond to the variable's truth value, i.e. R for true and L for false. Using Lemma 3, the boolean state of the variable gadget is transmitted to all transmitter gadgets associated to it. Each clause is realizable and so for every clause, there

exists one true literal in the clause corresponding to a variable by Lemma 2. If every clause has some true literal, then the corresponding 3-CNF boolean formula is satisfiable. □

Modified Auxilary Construction. Recall that in Theorem 1 we want to show that it is strongly NP-hard to decide whether a polygonal linkage whose hinge graph is a tree can be realized with counter-clockwise orientation. We modify the auxiliary construction allowing all polygons to move freely, and by adding extra polygons and hinges so that the hinge graph becomes a *tree*, and the size of the construction remains polynomial. The auxiliary construction is based on a polynomial sized area of the hexagonal grid, using obstacle hexagons of side lengths $N(n,m)$, unit hexagons (of side length 1), and small hexagons of side length $\frac{1}{3}$. We modify it in five steps as follows:

1. Move the obstacle hexagons apart such that the width of each corridor increases from $\sqrt{3}$ to $\sqrt{3}+1/(100N)$.
2. Replace the unit segment in each clause gadget by a skinny rhombus of diameter $\sqrt{1+(100N)^{-2}}$ and width $1/(100N)$.
3. Enclose the regular hexagon region J containing all gadgets by a *frame* of 6 congruent regular hexagons, as shown in Fig. 1.14(a), hinged together in a path.
4. Connect the frame and the obstacles in J into a simply connected polygonal linkage: in each obstacle hexagon, the bottom side is adjacent to the frame or to a corridor. Introduce a hinge at the midpoint of one such side in each obstacle hexagon. If this side is adjacent to the frame, then attach the hinge to the frame. Otherwise, the hinge is attached to a new *connector* polygon: a skinny rhombus of diameter 1 and width $\frac{1}{100N}$. The far corner of each rhombus is hinged to the unit hexagon in the middle of the corridor at shown in Figure 1.14(b).
5. The construction so far constains rows and columns of obstacle hexagons. Every other column of obstacle hexagons is hinged to the bottom side of the perimiter of J.

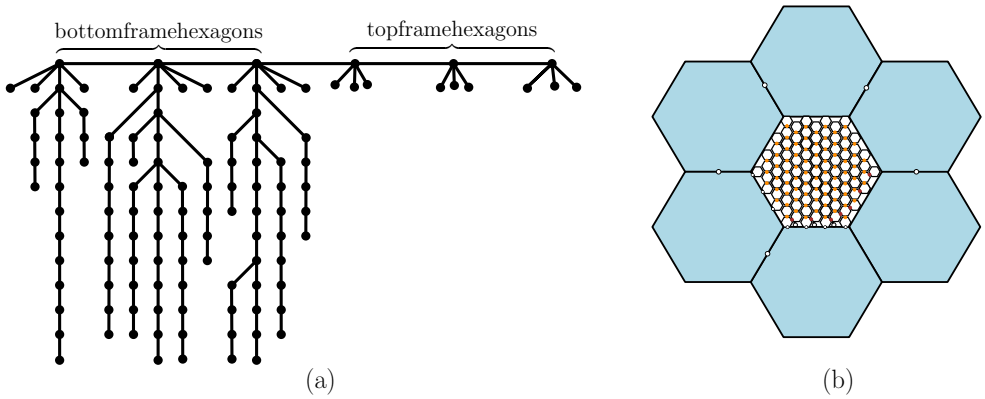

Figure 1.12: (a) illustrates a tree corresponding to the modified auxilary construction in (b). On the left half of the tree, we have the bottom most frame hexagons and the the hexagons in the interior of J as children of the the bottom frame hexagons. The top most frame hexagons only have the half sized hexgons attached to them. (b) is the corresponding modified auxilary construction.

These bottom most obstacle hexagons have a hinge point on its side. The columns that do not have an obstacle hexagon hinged to the perimeter of J has a half-sized hexgon hinged to the perimeter of J and a locked flag with no state to the first obstacle hexagon above it (See Figure 1.13).

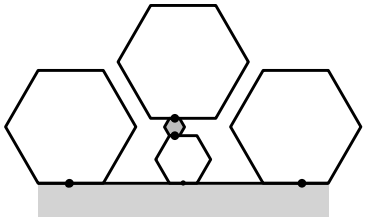

Figure 1.13: In this figure we illustrate the bottom of the perimeter of J with three obstacle hexagons, a half sized hexagon, and a locked flag whose hinge points lock the flag's state (becoming stateless).

We obtain a simply connected polygonal linkage. We now allow the obstacle hexagons to move freely, and call their original fixed position *canonical*. (3) We may assume without loss of generality that the frame is at its original position. It is enough to show that the obstacle hexagons are still confined to an $1/N$-neighborhood of their canonical position, then it follows that the polygonal linkage is realizable if and only if Φ is satisfiable.

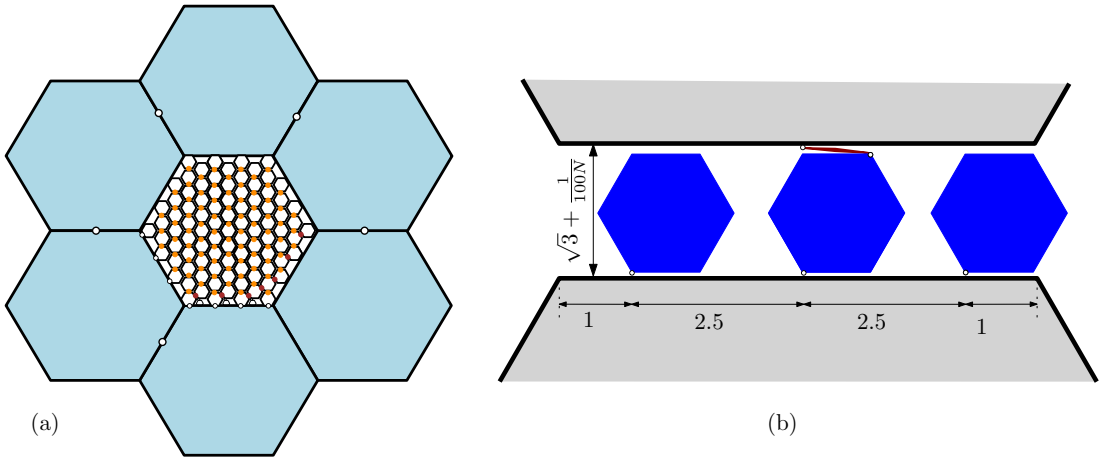

Figure 1.14: (a) A frame (built of 6 hinged regular hexagons) encloses a hexagonal tiling, and vertical paths connect all obstacle hexagons to the frame. (b) A corridor is widened to $\sqrt{3}+\frac{1}{N^2}$. A connection between two adjacent obstacle hexagons is established via a skinny rhombus.

The position of each hexagon can be defined by the isometry from its canonical position; an isometry is given by the triple (α,β,δ) where α is a counter clockwise rotation about the center of the hexagon and (β,δ) is a translation vector. Canonical position would have each obstacle hexagon's position as $(0,0,0)$.

Lemma 5. *Let P be a polygonal linkage obtained from the modified auxilary construction. In every realization of P, the obstacle polygons are close to canonical position such that*

Lemma 5 serves as assurance that once a boolean formula of P3SAT is encoded into an arbitrary realization of the modified auxilary construction, the information of the boolean formula is preserved regardless of the positioning of the gadgets and components in the construction. This quality shows that the information is stable and preserved in an arbitrary realization of the modified auxilary construction.

Proof. We need to show that the modified auxilary construction could not deform in such a way that any information the construction encodes is lost or modified and the functionality of the gadgets within the construction behave as stated in the description. For example, in Figure 1.15, we have a column of obstacle hexagons veering off ℓ.

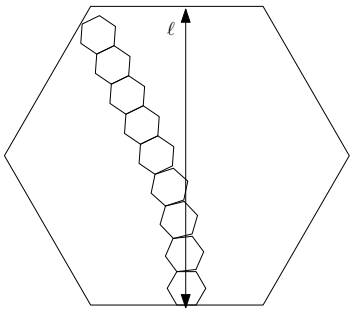

Figure 1.15: This figure depicts a column of obstacle hexagons rotated such that the obstacle hexagons veer of the vertical line ℓ.

This is an example of extreme angular rotation that should not occur over a vertical stack of hexagons. If a P3SAT boolean formula were encoded into such a realization, the information encoded could be lost by the extreme angular rotation of the obstacle hexagons.

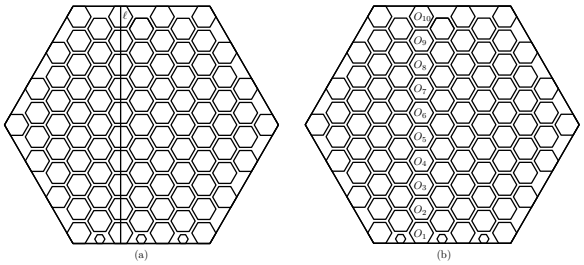

Figure 1.16: (a) depicts a column of obstacle hexagons O_1, ..., O_{10} along the vertical line ℓ; (b) identifies obstacle hexgons O_1, ..., O_{10} in (a).

Without loss of generality, we can identify a column of obstacle hexagons O_i along a vertical line ℓ (See Figure 1.16). In this proof, unless otherwise specified, we assume that the argument refers to a column that starts and ends with an obstacle hexagon. In total there will be $u+1$ number of obstacle hexagons and u corridors in a column. Note that:

$$\begin{aligned} u &= \tfrac{J_h(z)}{2} - \tfrac{1}{2} \\ &= \tfrac{1}{2}(6z+1-1) \\ &= 3z \\ &= 12s \end{aligned}$$

where J_h is defined in Equation 1.1.

The width of a skinny rhombus in canonical position is $\frac{1}{100N}$. The obstacle hexagon has height of $2N(n,m)\sqrt{3}$, and the flag is of height $\sqrt{3}$. The height $H(n,m)$ (and ℓ in Figure 1.17(a)) can be expressed as a sum of the heights of the corridors and obstacle polygons:

$$(u+1)2N\sqrt{3} + u\left(\sqrt{3} + \frac{1}{100N}\right)$$

which reducest to:

$$\begin{aligned} (u+1)2N\sqrt{3} + u\left(\sqrt{3} + \frac{1}{100N}\right) &= (12s+1)2\frac{5t-1}{2}\sqrt{3} + 12s\left(\sqrt{3} + \frac{1}{100\frac{5t-1}{2}}\right) \\ &= (12s+1)(5t-1)\sqrt{3} + 12s\left(\sqrt{3} + \frac{1}{250t-50}\right) \end{aligned}$$

$$H(n,m) = (12s+1)(5t-1)\sqrt{3} + 12s\left(\sqrt{3} + \frac{1}{250t-50}\right) \tag{1.4}$$

The cross section of the corridor must have a minimum height of $\sqrt{3}$ everywhere. Otherwise will result in overlapping polygons.

Angular Rotation α. First we show that the angular rotation of the obstacle hexagons with respect to canonical position is small. We first look at the relative angular difference between two adjacent obstacle polygons

$$|\alpha_i - \alpha_{i+1}|.$$

Given an arbitrary instance of a modified auxilary construction, consider O_i, O_{i+1}, and the corridor between O_i and O_{i+1} (see Figure 1.17 for illustration).

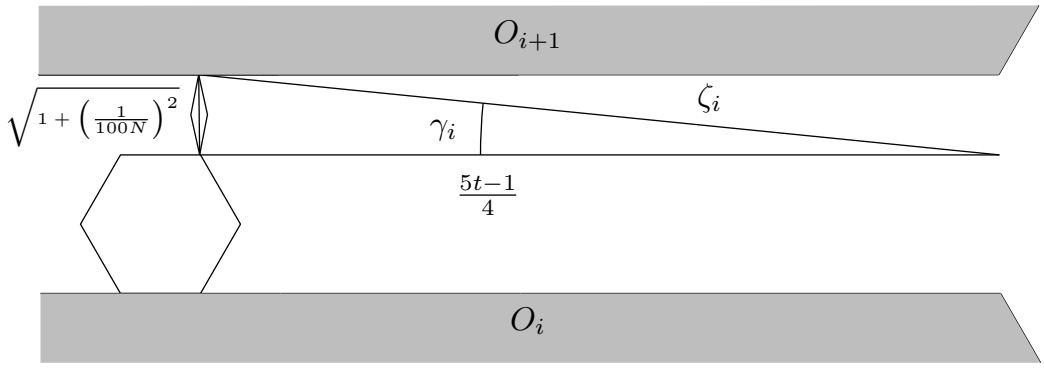

Figure 1.17: The obstacle hexagon here is in noncanonical position, and showing the side lengths adjacent to α_i.

In Figure 1.16(a) we see ℓ in the center of the column of obstacle hexagons. Our goal is to show that the column of hexagons cannot tilt in the manner shown in Figure 1.15 where the column veers greatly into the space occupied by other corridors and obstacle hexagons. The cross section of an arbitrary corridor must have a height of at least $\sqrt{3}$ everywhere. Otherwise, a flag would overlap with an obstacle hexagon; it would no longer remain a realization since the height of a flag is $\sqrt{3}$. In Figure 1.17, we illustrate an obstacle hexagon, its upper corridor with the flag that has the hinge to the skinny rhombus. The skinny rhombus has length $\sqrt{1+(100N)^{-2}}$. The rhombus is hinged at the midpoint of the upper side of the corridor. The length from a corridor's midpoint to one end of the corridor is $\frac{5t-1}{4}$. γ_i is the angle between ζ_i and the horizontal axis at the

height of the flag ($i = 1, 2, \ldots, u$). The bound of γ_i is:

$$\begin{aligned}
\gamma_i &\leq \tan^{-1}\left(\frac{\sqrt{1+\left(\frac{1}{100N}\right)^2}}{\frac{5t-1}{4}}\right) \\
&= \tan^{-1}\left(\frac{4\cdot\sqrt{1+\frac{1}{(100N)^2}}}{5t-1}\right) \\
&\leq \frac{4\cdot\sqrt{1+\frac{1}{(100N)^2}}}{5t-1} \\
&\leq \frac{\sqrt{16+\frac{16}{(100N)^2}}}{10N^3-6} \\
&\leq \frac{5}{10N^3-6} \\
&\leq \frac{5}{10N^3-10} \\
&\leq \frac{1}{2\left(N^3-1\right)} \\
&\leq \frac{1}{2\left(\frac{5t-1}{2}\right)^3-1} \\
&\leq \frac{4}{(5t-1)^3-4} \\
&\leq \frac{4}{\left(5s^k-1\right)^3-4} \\
&\leq \frac{4}{125s^{3\kappa}-75s^{2\kappa}+15s^{\kappa}-5}
\end{aligned} \tag{1.5}$$

Inequality 1.5 uses the first term Maclaurin series of $\tan^{-1}$. Thus the relative rotational difference between adjacent obstacle hexagons is

$$|\alpha_i - \alpha_{i+1}| \leq \frac{4}{125s^{3\kappa}-75s^{2\kappa}+15s^{\kappa}-5} \tag{1.6}$$

The relative difference between α_i and α_{i+1} is small. The bottom most obstacle hexagon is hinged to the frame (see Figure 1.13 for illustration). This implies that $\alpha_1 = 0$ and

$$|\alpha_1 - \alpha_2| = |\alpha_2| \leq \frac{4}{125s^{3\kappa}-75s^{2\kappa}+15s^{\kappa}-5}.$$

There are a total of u obstacle hexagons in a column with possibly up to $u-1$ nonzero obstcle hexagons rotations. We can derive 1) a bounded sum of rotational displacement over a column of obstacle hexagons:

$$\sum_{i=1}^{u-1} |\alpha_i - \alpha_{i+1}| \leq \frac{4(12s-1)}{125s^{3\kappa}-75s^{2\kappa}+15s^{\kappa}-5} \tag{1.7}$$

and 2) derive the maximum rotational displacement at the i^{th} obstacle hexagon:

$$\begin{aligned}
\alpha_i &\leq \sum_{j=1}^{i} \frac{4j}{125s^{3\kappa} - 75s^{2\kappa} + 15s^{\kappa} - 5} \\
&\leq \frac{4}{125s^{3\kappa} - 75s^{2\kappa} + 15s^{\kappa} - 5} \sum_{j=1}^{i} j \\
&\leq \frac{4}{125s^{3\kappa} - 75s^{2\kappa} + 15s^{\kappa} - 5} \cdot \frac{i^2 + i}{2} \\
&\leq \frac{2(i^2 + i)}{125s^{3\kappa} - 75s^{2\kappa} + 15s^{\kappa} - 5} \\
&\leq \frac{2(u^2 + u)}{125s^{3\kappa} - 75s^{2\kappa} + 15s^{\kappa} - 5} \\
&\leq \frac{2(144s^2 + 12s)}{125s^{3\kappa} - 75s^{2\kappa} + 15s^{\kappa} - 5} \\
&\leq \frac{288s^2 + 24s}{125s^{3\kappa} - 75s^{2\kappa} + 15s^{\kappa} - 5}
\end{aligned}$$

For any i, the bound for α_i:

$$\alpha_i \leq \frac{288s^2 + 24s}{125s^{3\kappa} - 75s^{2\kappa} + 15s^{\kappa} - 5} \tag{1.8}$$

Vertical Displacement δ When an obstacle hexagon is rotated by α_i, the height of the obstacle hexagon becomes $h \sec \alpha_i$ where h is the canonical height of the obstacle hexagon (see Figure 1.18 for reference). Figure 1.18 shows the geometry of a rotated obstacle hexagon.

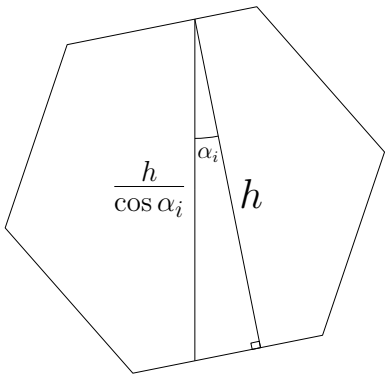

Figure 1.18: This figure shows a right triangle with angle α_i and sides of length h and $\frac{h}{\cos \alpha_i}$.

To show that the vertical displacement from canonical position is small, we first consider a column of obstacle hexagons in canonical position (see Figure 1.16 for illustration). For canonical position, the j^{th} obstacle has $\delta_j = 0$.

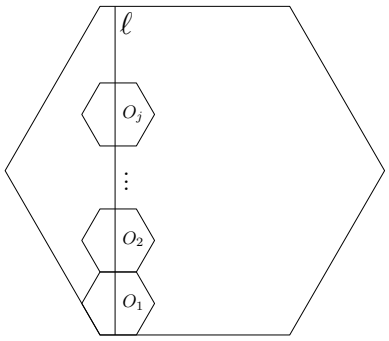

Figure 1.19: This illustration is of a column of obstacle hexagons in canonical position along a vertical line segment ℓ.

From Equation 1.4, we know the exact height of ℓ in terms of the heights of the corridors and obstacle hexagons in canonical position. Consider the first j terms for the height of the column of obstacle hexagons and corridors for an arbitrary construction with angular rotation and vertical displacement for *one* obstacle hexagon $|\delta_v| > 0$, where $j = 2, \cdots, u+1$ and $1 < v \leq j$.

$$\begin{aligned}
\sum_{i=1}^{j}\left(2\sqrt{3}N\sec(\alpha_i)\right)+\delta_v+(j-1)\left(\frac{1}{100N}+\sqrt{3}\right) &\leq j\cdot 2N\sqrt{3}+(j-1)\cdot\left(\frac{1}{100N}+\sqrt{3}\right)\\
2\sqrt{3}N\sum_{i=1}^{j}\sec(\alpha_i)+\delta_v &\leq j\cdot 2\sqrt{3}N\\
\sum_{i=1}^{j}\sec(\alpha_i)+\delta_v &\leq j\\
\delta_v &\leq j-\sum_{i=1}^{j}\sec(\alpha_i)\\
\delta_v &\leq j-\left(j-\sum_{i=1}^{j}\frac{\alpha_i^2}{2}\right)\\
\delta_v &\leq \sum_{i=1}^{j}\frac{\alpha_i^2}{2}
\end{aligned}$$

Using Inequalities 1.7 and 1.8, we derive the following result:

$$\begin{aligned}
\textstyle\sum_{i=1}^{j}\frac{\alpha_i^2}{2} &\leq \tfrac{1}{2}\textstyle\sum_{i=1}^{j}\left(\frac{288s^2+24s}{125s^{3\kappa}-75s^{2\kappa}+15s^{\kappa}-5}\right)^2\\
&\leq \tfrac{1}{2}\cdot\left(\frac{288s^2+24s}{125s^{3\kappa}-75s^{2\kappa}+15s^{\kappa}-5}\right)^2\cdot j\\
&\leq \tfrac{1}{2}\cdot\left(\frac{288s^2+24s}{125s^{3\kappa}-75s^{2\kappa}+15s^{\kappa}-5}\right)^2\cdot u\\
&\leq \tfrac{1}{2}\cdot\left(\frac{288s^2+24s}{125s^{3\kappa}-75s^{2\kappa}+15s^{\kappa}-5}\right)^2\cdot 12s\\
&\leq \frac{6s\left(288s^2+24s\right)^2}{\left(125s^{3\kappa}-75s^{2\kappa}+15s^{\kappa}-5\right)^2}
\end{aligned}$$

Thus we finally say that the bound for δ_v, where $1 < v \leq j \leq u$, is small:

$$\delta_v \leq \frac{6s\left(288s^2+24s\right)^2}{\left(125s^{3\kappa}-75s^{2\kappa}+15s^{\kappa}-5\right)^2} \tag{1.9}$$

Horizontal Displacement β Next we show that the horizontal displacement of an obstacle hexagon is small. Note that there is no horizontal displacement of obstacle hexagons hinged to the frame; their positions are fixed. Similarly, obstacle hexagons hinged to half hexagons near the bottom of the frame do not have horizontal displacement because their positions are also fixed. Without loss of generality, $\beta_{1,j} = 0$ for all j in a modified construction.

To illustrate the range of displacement an obstacle hexagon, we consider the range of motion the obstacle hexagon's skinny rhombus, its rotational displacement, and vertical displacement. The bound of the horizontal displacement will be limited by the bound of the vertical displacement δ_i. The vertical displacement formed by the i^{th} skinny rhombus' motion is δ_{ω_i}; the vertical displacement formed by the i^{th} obstacle hexagon's rotational displacement is δ_{α_i}.

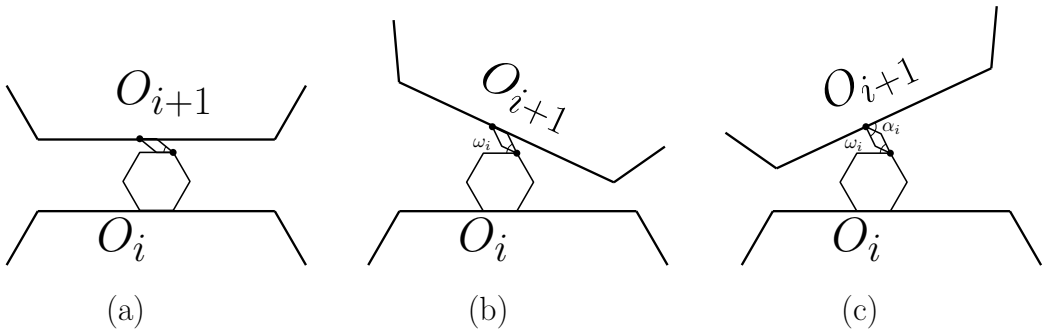

Figure 1.20: (a) A pair of vertically adjacent obstacle hexagons and their corresponding corridor in canonical position. (b) shows the same obstacle hexagons and corridors with the exception that the skinny rhombus is not in cannonical position. (c) is the same as (b) with the exception that the obstacle hexagon O_{i+1} has rotation displacement.

The skinny rhombus hinged beneath an obstacle hexagon can rotate on its hinge with the flag. The angle formed between the diameter segment of the rhombus at canonical position to the position of the diameter segment in a given configuration is ω. Figure 1.20(a) shows the cannonical position of all objects where $\omega_i = 0$. Figure 1.20(b) illustrates some range of motion ω_i that a skinny rhombus can rotate on its hinge with a flag. Figure 1.20(c) shows a rotational displacement of O_{i+1}. In the case that $\omega_i > \frac{\pi}{2}$ the rotational displacement α_i creates a positive vertical displacement β_{α_i} with respect to the center of its corresonding obstacle hexagon.

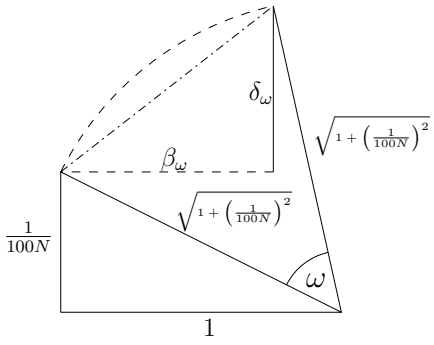

Figure 1.21: The vertical displacement δ_ω and horizontal displacement β_ω created from the skinny rhombus rotation ω.

First let's consider the case when $\omega \leq \frac{\pi}{2}$. In 1.21, the vertical and horizontal displacement formed by the angular rotation ω of the skinny rhombus is shown. The maximal displacement of the i^{th} vertical displacement is δ_i; thus $\delta_{\omega_i} \leq \delta_i$. The right triangle formed from β_ω and δ_ω has a maximal hypotenuse length of $\sqrt{2}\delta_\omega$. Because this right triangle is derived from the circular segment about the skinny rhombus' hinge point and the

limitation of the maximal displacement of δ_ω, the hypotenuse has a maximal feasible distance of $\sqrt{\delta_\omega^2+\delta_\omega^2}$. The horizontal displacement β_ω is bounded as such:

$$\beta_\omega \leq \delta_\omega \leq \delta_i \leq \frac{6s\left(288s^2+24s\right)^2}{\left(125s^{3\kappa}-75s^{2\kappa}+15s^{\kappa}-5\right)^2} \tag{1.10}$$

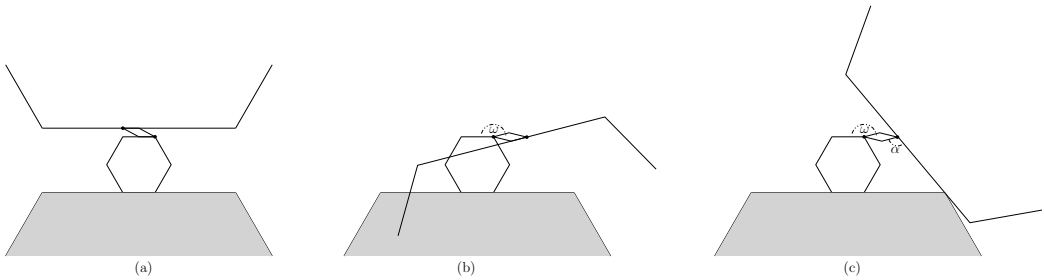

Figure 1.22: (a)A pair of obstacle hexagons, their corresponding corridor with a flag and skinny rhombus; all components are in cannonical position. (b) shows the maximal horizontal displacement from ω and no obstacle hexagon rotation. (c) shows a maximal horizontal displacement from ω and obstacle hexagon rotation α.

For the case that $\omega_i > \frac{\pi}{2}$, we may result in some cases where polygons may overlap in their interiors. We illustrate some infeasible realizations with horizontal displacement to evaluate the length of β_α, the horizontal displacement with respect to the rotation of an obstacle hexagon. We then continue to show that $\beta_\alpha = 0$ for all feasible realizations and conclude that the bound of horizontal displacement is infact the Inequality 1.10.

Figure 1.22(b) shows maximal horizontal displacement with respect to ω, β_ω. The corresponding skinny rhombus in Figure 1.22(b) is rotated to lie parallel with the corridor yielding a horizontal displacement $\beta_\omega = \sqrt{1+(100N)^{-2}}$. Figure 1.22(c) adds further horizontal displacement to the obstacle hexagon O_{i+1} by rotating the O_{i+1} by α.

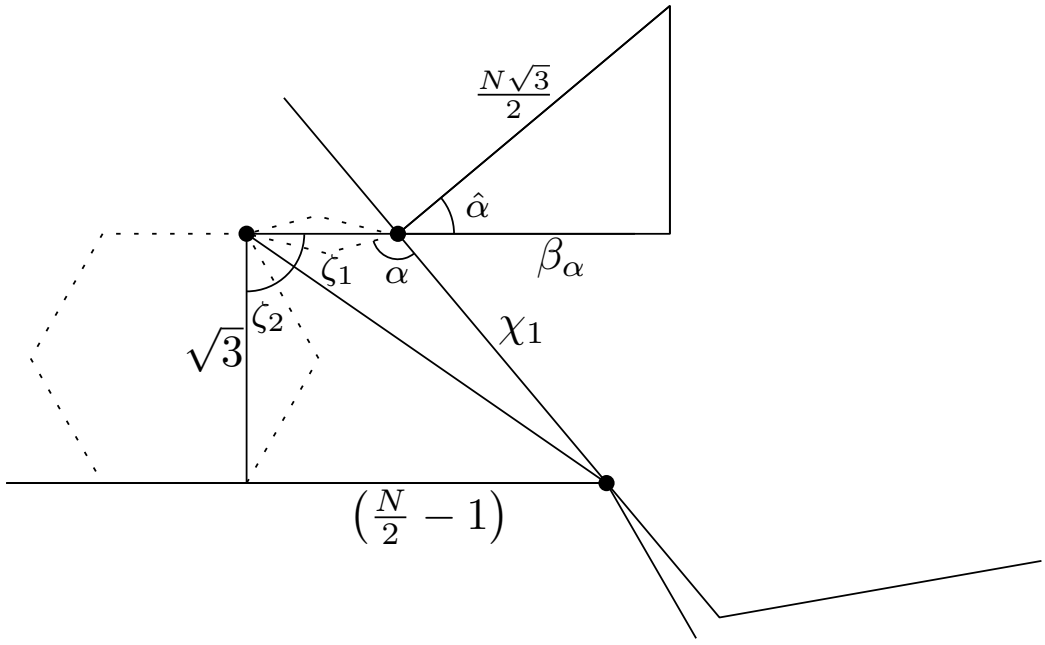

Figure 1.23: A more detailed illustration of Figure 1.22(c).

Figure 1.23 illustrates Figure 1.22(c) in more detail. The equations below serve as an aid to the reader to derive the maximal horizontal displacement of β_α:

$$\begin{aligned}
\zeta_2 &= \tan^{-1}\left(\frac{\frac{N}{2}-1}{\sqrt{3}}\right) \\
\zeta_1 &= \frac{\pi}{2}-\zeta_1 \\
\chi_1 &= \sqrt{(1+(100N)^{-2})+\left(\left(\frac{N}{2}-1\right)^2+3\right)-2\cdot\left(\left(\frac{N}{2}-1\right)^2+3\right)\cdot(1+(100N)^{-2})\cdot\cos\zeta_1} \\
\hat{\alpha} &= \alpha-\frac{\pi}{2} \\
\beta_\alpha &= \frac{N\sqrt{3}}{2}\cos\hat{\alpha}
\end{aligned}$$

Lemma 6. *There are no possible realizations when $\omega \geq \frac{\pi}{2}$.*

Proof. In this case the range of ω is $\frac{\pi}{2} \leq \omega \leq \left(\frac{4\pi}{3}-\hat{\omega}\right)$ where $\hat{\omega} = \tan^{-1}\left(\frac{1}{50N}\right)$ is the acute angle in the interior of the skinny rhombus. The upperbound $\left(\frac{4\pi}{3}-\hat{\omega}\right)$ is the case when the skinny rhombus' side is touching its flag's upper right side. When $\omega = \frac{\pi}{2}$, the height of the hinge point of the obstacle hexagon and skinny rhombus from the bottom of the corridor is $1+\sqrt{3}$ which is less than the half length of the side of the obstacle hexagon $\frac{N}{2}$. Thus we have an overlap of obstacle hexagons; namely an of the obstacle hexagons shown in 1.22(a) and the obstacle hexagon to the right of the corresponding corridor or if α is large enough, only the obstacle hexagon to the right of the corresponding corridor. When $\omega > \frac{\pi}{2}$ the height of the hinge point of the obstacle hexagon and skinny rhombus is lowered and results in overlap of obstacle hexagons; namely an of the obstacle hexagons shown in 1.22(a) and the obstacle hexagon to the right of the corresponding corridor or if α is large enough, only the obstacle hexagon to the right of the corresponding corridor (for example see Figure 1.22(c)). □

By Lemma 6 we have that ω must be less than $\frac{\pi}{2}$ and thus $\beta_\alpha = 0$ and the horizontal displacement is bounded by β_ω. Earlier we've shown that β_ω is bounded in Inequality 1.10 and so β is bounded by the same inequality.

□

Bibliography

[1] James A Storer. On minimal-node-cost planar embeddings. *Networks*, 14(2):181–212, 1984.

[2] R Tamassia and IG Tollis. Efficient embedding of planar graphs in linear time. In *Proc. IEEE Int. Symp. on Circuits and Systems*, pages 495–498, 1987.